First *in situ* Raman study of vanadium oxide based SO_2 oxidation supported molten salt catalysts

I. Giakoumelou [a], R.M. Caraba [b], V.I. Parvulescu [b], and S. Boghosian [a,*]

[a] *Department of Chemical Engineering, University of Patras and Institute of Chemical Engineering and High Temperature Chemical Processes (FORTH/ICE-HT), PO Box 1414, University Campus, GR-26500 Patras, Greece*

[b] *University of Bucharest, Department of Chemical Technology and Catalysis, B-dul Regina Elisabeta 4-12, Bucharest 70346, Romania*

Received 13 August 2001; accepted 10 October 2001

In situ Raman spectroscopy at temperatures up to 500 °C is used for the first time to identify vanadium species on the surface of a vanadium oxide based supported molten salt catalyst during SO_2 oxidation. Vanadia/silica catalysts impregnated with Cs_2SO_4 were exposed to various $SO_2/O_2/SO_3$ atmospheres and *in situ* Raman spectra were obtained and compared to Raman spectra of unsupported "model" V_2O_5–Cs_2SO_4 and V_2O_5–$Cs_2S_2O_7$ molten salts. The data indicate that (1) the V^V complex $V^VO_2(SO_4)_2^{3-}$ (with characteristic bands at 1034 cm^{-1} due to $\nu(V{=}O)$ and 940 cm^{-1} due to sulfate) and Cs_2SO_4 dominate the catalyst surface after calcination; (2) upon admission of SO_3/O_2 the excess sulfate is converted to pyrosulfate and the V^V dimer $(V^VO)_2O(SO_4)_4^{4-}$ (with characteristic bands at 1046 cm^{-1} due to $\nu(V{=}O)$, 830 cm^{-1} due to bridging S–O along S–O–V and 770 cm^{-1} due to V–O–V) is formed and (3) admission of SO_2 causes reduction of V^V to V^{IV} (with the $\nu(V{=}O)$ shifting to 1024 cm^{-1}) and to V^{IV} precipitation below 420 °C.

KEY WORDS: molten salt catalysts; V_2O_5 catalyst; *in situ* Raman spectra; SO_2 oxidation; vanadium oxosulfato complexes

1. Introduction

The catalytic oxidation of SO_2 to SO_3 plays a key role in a number of industrial processes, which due to the associated sulfur oxide emissions have significant environmental impact. Although the main source of SO_2 emissions to the atmosphere is the coal-fired power generation, large amounts of SO_2 are also emitted from sulfuric acid manufacturers and smelters of non-ferrous metals. Production of sulfuric acid is currently performed not only from traditional sulfuric acid manufacturers but also from NO_x and SO_x removal stations, combined with SCR technology like, *e.g.*, in the so-called Haldor–Topsøe SNOX process [1]. The catalyst used for sulfuric acid production catalyzing the reaction

$$SO_2 + (1/2)O_2 \rightarrow SO_3$$

contains its active phase in a molten salt which is distributed in the pores of an inert silica support and is the most important supported liquid-phase (SLP) catalyst [2]. The catalyst is usually made by calcination of silica (diatomaceous earth), vanadium pentoxide (or other vanadium precursors) and alkali promoters (usually in the form of sulfates) with an alkali-to-vanadium ratio between 2 and 5 [2,3]. During SO_2 oxidation, large amounts of SO_3 are taken up by the catalyst, of which the active phase is best simulated by vanadium oxide dissolved in alkali pyrosulfate thereby giving rise to formation of vanadium oxosulfato complexes [3].

In situ real-time spectroscopic characterization of catalytic active centers in vanadium oxide based SO_2 oxidation *supported molten salt* catalysts under gas and temperature conditions of practical importance has been a long-sought goal in catalysis [3]. On the other hand, the SO_2 oxidation over conventional supported *solid metal oxide* SCR catalysts has recently attracted interest [4–6] but the *in situ* Raman studies performed on such *solid metal oxide* catalysts are undertaken mainly in conditions simulating the SCR of NO by NH_3 in the absence of SO_2 [7–10]. However, the results of these studies by no means relate to the structure of the molten salt catalyst during SO_2 oxidation.

Recently, high temperature Raman spectroscopy has been used to establish the structural and vibrational properties of vanadium oxosulfato complexes present in the unsupported V_2O_5–$Cs_2S_2O_7$–Cs_2SO_4/O_2 [11], V_2O_5–M_2SO_4/O_2 (M = K or Cs) [12] and V_2O_5–$M_2S_2O_7$–M_2SO_4/SO_2–O_2 (M = K or Cs) [13] molten salt/gas systems. The obtained information contributed significantly in achieving progress on the mechanistic understanding of SO_2 oxidation catalysts [3] and prepared the grounds for the present work. The above molten salt systems simulate the active phase, which is distributed in the pores of the SLP catalysts used for sulfuric acid production and removal of SO_2 from flue gas [14].

The present article reports the *first in situ* Raman evidence for identifying vanadium species on the surface of a vanadium oxide based SO_2 oxidation molten salt catalyst. Furthermore, to our knowledge, there has been no previous report of *in situ* Raman study of *any* catalysts in SO_2 atmosphere.

---

[*] To whom correspondence should be addressed. E-mail: bogosian@iceht.forth.gr

2. Experimental

2.1. Catalyst preparation and characterization

The samples studied were vanadia–silica and Cs-promoted vanadia–silica mesoporous catalysts prepared by a sol–gel process using tetraethylorthosilicate (Aldrich >99% pure), vanadylacetylacetonate (Aldrich, 95%) and Cs_2SO_4 (Merck, >99.5%) as precursors [15]. Results presented here concern one of the Cs-promoted vanadia–silica catalysts which exhibited the highest catalytic activity amongst all samples studied [15]. This mesoporous vanadia–silica catalyst had a BET surface area (N_2 adsorption at 77 K) of 533 $m^2\,g^{-1}$, a mean pore radius of 3.6 nm, a 6.5 wt% vanadium content based on ICP-AES analysis and a Cs : V ratio of 3 : 1 resulting from impregnation of the catalyst with Cs_2SO_4.

2.2. In situ Raman furnace and Raman spectra

Approximately 150 mg of the catalyst were pressed into a self-supporting wafer, which was mounted on a stainless-steel adjustable holder in the center of the *in situ* Raman furnace. The Raman furnace is a kanthal-wound double-wall quartz glass tube furnace mounted on an *xyz* plate and possesses gas inlets and outlets as well as a thermocouple sheath in contact with the catalyst sample holder and will be described in detail elsewhere [16]. The gases used were SO_2 (Matheson, Union Carbide 99.98% anhydrous), N_2 (L'Air Liquide, 99.999%) and O_2 (L'Air Liquide, 99.999%) and were mixed by using thermal mass flowmeters (Brooks Instr. Model 5850E). The gas feed consisted of 0.4% SO_2 and 4% O_2 in a balance of N_2 at a total feed flow rate of 50 cm^3/min corresponding to a space velocity of 35 h^{-1}.

Raman spectra were excited by using the 488.0 nm line of a Spectra Physics 164 argon ion laser, which was focused on the sample by a cylindrical lens. The power of the laser was adjusted at 60 mW, measured before its entrance in the Raman furnace. The scattered light was collected at 90° (horizontal scattering plane), analyzed with a 0.85 m Spex 1403 double monochromator and detected by a $-20\,^{\circ}C$ cooled RCA photomultiplier equipped with EG&G photon counting electronics.

3. Results and discussion

The catalyst was calcined in the Raman furnace by heating gradually at 100, 300, 400 and 500 °C (for 1 h at each temperature) under a flow of oxygen and *in situ* Raman spectra were recorded after one hour of exposure to O_2 at each temperature. Heating of the catalyst containing vanadium oxide and cesium sulfate under oxygen at 500 °C is expected to lead to a molten salt, which is distributed in the silica support [12]. It has been shown that a 2 : 1 $Cs_2SO_4 : V_2O_5$ mixture melts below 450 °C and contains $VO_2(SO_4)_2^{3-}$ and VO_3^- units in chain-like and network-like configurations, whereas further addition of sulfate results in precipitation of crystalline Cs_2SO_4 [12].

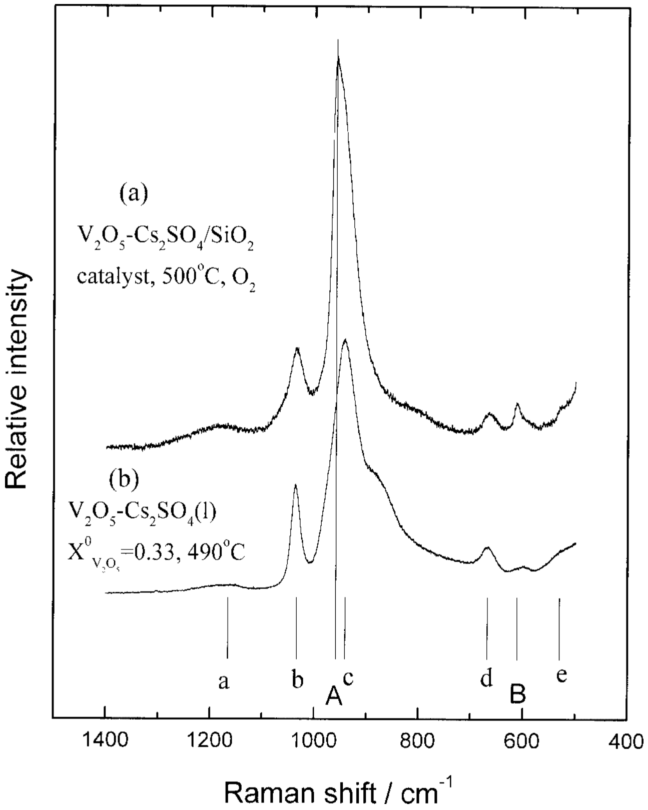

Figure 1. (a) *In situ* Raman spectrum of V_2O_5/SiO_2 (6.5 wt% V) impregnated with Cs_2SO_4 (Cs : V = 3 : 1) at 500 °C under O_2, calcined in the Raman furnace. Laser wavelength, $\lambda_0 = 488.0$ nm, laser power w = 60 mW, spectral slit width sww = 8 cm^{-1}, scan speed ss = 0.2 $cm^{-1}\,s^{-1}$, time constant $\tau = 1$ s. (b) Raman spectrum V_2O_5–Cs_2SO_4 molten mixture with $X^0_{V_2O_5} = 0.33$ at 490 °C (reproduced from [12]).

Figure 1(a) shows *in situ* Raman spectra taken at 500 °C under O_2 right after the calcination process and exhibits peaks at ~1168 (weak, broad), 1034 (strong), 960 (very strong, sharp, with a shoulder in its low frequency side at ~940 cm^{-1}), 668 (medium), 611 (medium, sharp) and 530 (weak) cm^{-1}. Significantly, the bands at 1170, 1034, 940, 668 and 530 cm^{-1} are known to originate from $VO_2(SO_4)_2^{3-}$, which is a product of the reaction of vanadium oxide and cesium sulfate [12], which can be written as

$$V_2O_5 + 2SO_4^{2-} \rightarrow 2VO_2(SO_4)_2^{3-} + VO_3^- \qquad (1)$$

The spectrum of the V_2O_5–Cs_2SO_4 molten mixture with $X^0_{V_2O_5} = 0.33$ (*i.e.*, Cs : V = 2 : 1) at 490 °C (reproduced from [12]) is shown in figure 1(b) to facilitate the comparison. Naturally, since the state of vanadium oxide present cannot be described accurately as V_2O_5, reaction (1) has to be considered only as a scheme accounting for the formation of molten $VO_2(SO_4)_2^{3-}$ at the catalyst surface. For the same reason it might be more appropriate to symbolize the second product of reaction (1) as VO_x. The sharp bands at 960 and 611 cm^{-1} observed in the spectrum of the freshly calcined catalyst (figure 1(a)) are due to the well known $\nu_1(SO_4^{2-})$ and

Table 1

Observed vibrational Raman wavenumbers (cm^{-1}) in *in situ* Raman spectra of Cs-promoted vanadia/silica catalyst and model molten salt mixtures[a]

Band notation (figure 1)	$V^VO_2(SO_4)_2^{3-}$ 490 °C [12]	V_2O_5–Cs_2SO_4/ calcined catalyst 500 °C, O_2	Assignments for catalyst (based on [12])	Band notation (figure 2)	$(V^VO)_2O(SO_4)_4^{4-}$ 450 °C [11]	V_2O_5–Cs_2SO_4/SiO_2 SiO_2 catalyst 380 °C, $SO_2 + O_2$	Assignments for catalyst (based on [11,12])
a	1166 w	1168 w	$V^VO_2(SO_4)_2^{3-}$ [b]	α	1176 m	1172 m	$(V^VO)_2O(SO_4)_4^{4-}$ [b]
				β	1047 s	1046 m	$\nu(V{=}O)$, $(V^VO)_2O(SO_4)_4^{4-}$
b	1036 s	1034 s	$\nu(V{=}O)$, $V^VO_2(SO_4)_2^{3-}$	b		1034 w, sh	$\nu(V{=}O)$, $V^VO_2(SO_4)_2^{3-}$
				γ	996 m	994 m	$\nu(S–O_t)$, $(V^VO)_2O(SO_4)_4^{4-}$
A		960 vs, sharp	$\nu_1(SO_4^{2-})$, Cs_2SO_4 (cr)				
c	941 s	940 s	$\nu(SO_4^{2-})$, $V^VO_2(SO_4)_2^{3-}$	c		939 m	$\nu(SO_4^{2-})$, $V^VO_2(SO_4)_2^{3-}$
	880 br						
				δ	825 s, br	830 s, br	$\nu(S–O_b)$, $(V^VO)_2O(SO_4)_4^{4-}$
				ε	765 m	770 m, br	$\nu(V–O–V)$, $(V^VO)_2O(SO_4)_4^{4-}$
						700 w	
				ζ	690 w	687 m	$(V^VO)_2O(SO_4)_4^{4-}$ [c]
d	666 m	668 m	$V^VO_2(SO_4)_2^{3-}$ [c]	η	669 w	666 m	$(V^VO)_2O(SO_4)_4^{4-}$, $V^VO_2(SO_4)_2^{3-}$ [c]
B		611 m, sharp	$\nu_4(SO_4^{2-})$, Cs_2SO_4 (cr)		611 w	616 w	$(V^VO)_2O(SO_4)_4^{4-}$ [c]
	603 w			θ	582 m	593 w	$(V^VO)_2O(SO_4)_4^{4-}$ [c]
e	533 w	530 w	$V^VO_2(SO_4)_2^{3-}$ [c]		486 m		
	407 s				393		
	279 w				302 s		
	226 s				196		

[a] Abbreviations: s = strong; m = medium; w = weak; v = very; sh = shoulder; br = broad.

[b] Assigned to $\nu_3(SO_4)$ split components.

[c] Assigned either to $\nu_4(SO_4)$ split components or $\nu(V–O–)$.

$\nu_4(SO_4^{2-})$ modes of the excess crystalline Cs_2SO_4 present since the Cs : V ratio of the catalyst sample is equal to 3 (*i.e.*, $X^0_{V_2O_5} = 0.25$) and it is known that for $X^0_{V_2O_5} < 0.33$ crystalline Cs_2SO_4 precipitates out [12]. Table 1 (columns 1–4) lists the Raman band wavenumbers and their assignments for the *in situ* Raman spectrum of the calcined catalyst under O_2 at 500 °C and includes the Raman frequencies of the molten $VO_2(SO_4)_2^{3-}$ complex for comparison.

One should expect to observe the group vibrations of VO^{3+} and SO_4^{2-} units of the $VO_2(SO_4)_2^{3-}$ V^V complex. The four sulfate fundamentals (ν_1–ν_4) for a tetrahedral T_d configuration span the following representation

$$\Gamma_{vib} = A_1(\nu_1) + E(\nu_2) + 2F_2(\nu_3 + \nu_4)$$

and are well known from Raman work on aqueous solutions: $\nu_1(A_1) \approx 980\ cm^{-1}$, $\nu_2(E) \approx 450\ cm^{-1}$, $\nu_3(F_2) \approx 1100\ cm^{-1}$ and $\nu_4(F_2) \approx 615\ cm^{-1}$ [17]. However, coordination of the sulfate ion and interactions with other ions are expected to shift the bands moderately, reduce the symmetry and lift the degeneracies of the ν_2, ν_3 and ν_4 modes. This behavior has already been observed in the Raman spectra of molten M_2SO_4–V_2O_5, $M_2S_2O_7$–V_2O_5 and $M_2S_2O_7$–M_2SO_4–V_2O_5 (M = K or Cs) mixtures [11–13]. Vertical lines in figure 1 mark the most prominent bands due to the various species present as follows: uppercase A, B denote bands due to crystalline Cs_2SO_4; lowercase a–e denote bands due to $VO_2(SO_4)_2^{3-}$ and the same notation is used in table 1. The band at 1034 cm^{-1} is due to the V^V=O terminal stretch of six-coordinated vanadium of $VO_2(SO_4)_2^{3-}$ and the shoulder band at 940 cm^{-1} is due to S–O terminal stretches of sulfate in $VO_2(SO_4)_2^{3-}$ [12]. The strong shoulder band at 880 cm^{-1} observed in the spectrum of the *molten salt mixture* (figure 1(b)) – and not in figure 1(a) – has previously [12] been assigned to S–O bridging modes along S–O–V chains of three-dimensional network-like $[VO_2(SO_4)_2]_n^{3n-}$ polymeric configurations formed in the unsupported molten salts [12]. Such extensive networking is not expected at the surface of the catalyst where the liquid/molten phase is distributed in the form of thin (100–1000 Å) layers/films [2].

Figure 2 shows the temperature dependence of *in situ* Raman spectra of the catalyst at SO_2/O_2 atmosphere (spectra (b)–(f)). The *in situ* spectrum of the calcined catalyst under O_2 at 500 °C is included for comparison (Figure 2(a)). Spectrum 2(b) is obtained after exposure of the sample to SO_2 and O_2 at 500 °C for 1 h. The retention time is sufficiently low to secure that SO_2 is converted to SO_3, which in turn reacts with crystalline sulfate forming molten pyrosulfate according to

$$SO_4^{2-} + SO_3 \rightarrow S_2O_7^{2-}$$

This results, as seen in figure 2(b), in disappearance of bands A and B at 960 $[\nu_1(SO_4^{2-})]$ and 611 $[\nu_4(SO_4^{2-})]$ cm^{-1}, which were due to crystalline sulfate. Moreover, the $S_2O_7^{2-}$ formed dissolves the residual vanadium(V) oxides present and the reaction taking place can be written as [11,13]

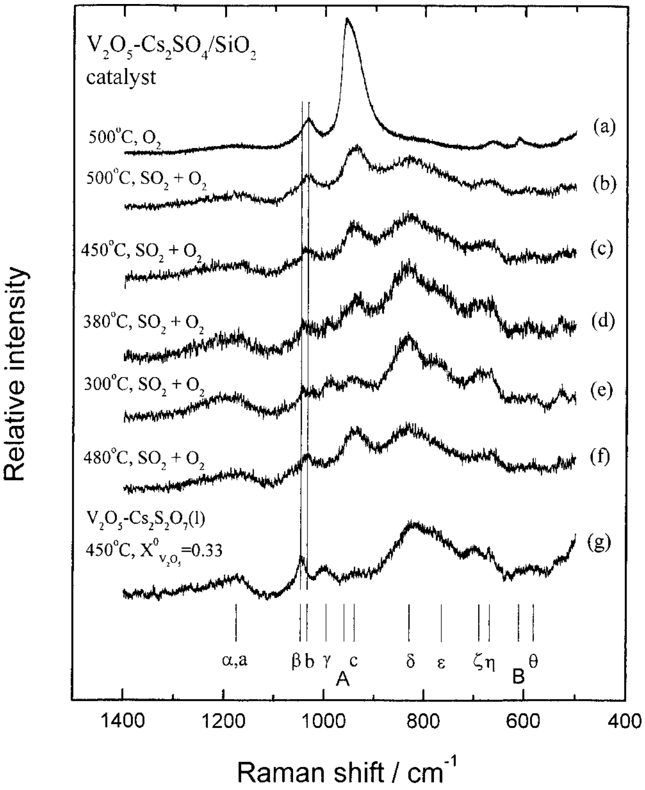

Figure 2. (a)–(f) *In situ* Raman spectra of V_2O_5/SiO_2 (6.5 wt% V) impregnated with Cs_2SO_4 (Cs : V = 3 : 1) recorded at temperatures and atmospheres listed by each spectrum. λ_0 = 488.0 nm, w = 60 mW, ssw = 8 cm^{-1}, ss = 0.2 cm^{-1} s^{-1}, τ = 1 s. (g) Raman spectrum of V_2O_5–$Cs_2S_2O_7$ molten mixture with $X^0_{V_2O_5}$ = 0.33 at 450 °C. Vertical lines mark the positions of the terminal V=O stretches due to $VO_2(SO_4)_2^{3-}$ (1034 cm^{-1}) and $(VO)_2O(SO_4)_4^{4-}$ (1047 cm^{-1}) [11,12].

$$V_2O_5 + 2S_2O_7^{2-} \rightarrow (VO)_2O(SO_4)_4^{4-} \qquad (2)$$

and indeed the characteristic 770/830 cm^{-1} strong and broad feature due to the molten dimeric $(VO)_2O(SO_4)_4^{4-}$ appears [11]. The 830 cm^{-1} band is due to bridging S–O along S–O–V and the 770 cm^{-1} band is due to V–O–V of the $(VO)_2O(SO_4)_4^{4-}$ molten complex [11,13], which is considered the active species in the catalytic cycle of SO_2 oxidation [3]. In order to facilitate the discussion, the spectrum of the $(VO)_2O(SO_4)_4^{4-}$ molten complex (*i.e.*, of the $V_2O_5-Cs_2S_2O_7$ molten mixture with $X^0_{V_2O_5} = 0.33$) at 450 °C is displayed in figure 2(g).

Lowering of the temperature to 450–380 °C under SO_2 and O_2 results in the following changes observed in the *in situ* Raman spectra shown in figure 2 (c) and (d): (i) gradual blue shift of the 1034 cm^{-1} band (band b) due to the V^V=O terminal stretch of $VO_2(SO_4)_2^{3-}$ to 1046 cm^{-1} (band β), where the V^V=O terminal stretch of $(VO)_2O(SO_4)_4^{4-}$ is known to occur [11–13]; (ii) appearance of bands at 994 and 687 (bands γ and ζ) due to terminal S–O stretch and $\nu_4(SO_4^{2-})$ split component of $(VO)_2O(SO_4)_4^{4-}$ [11];

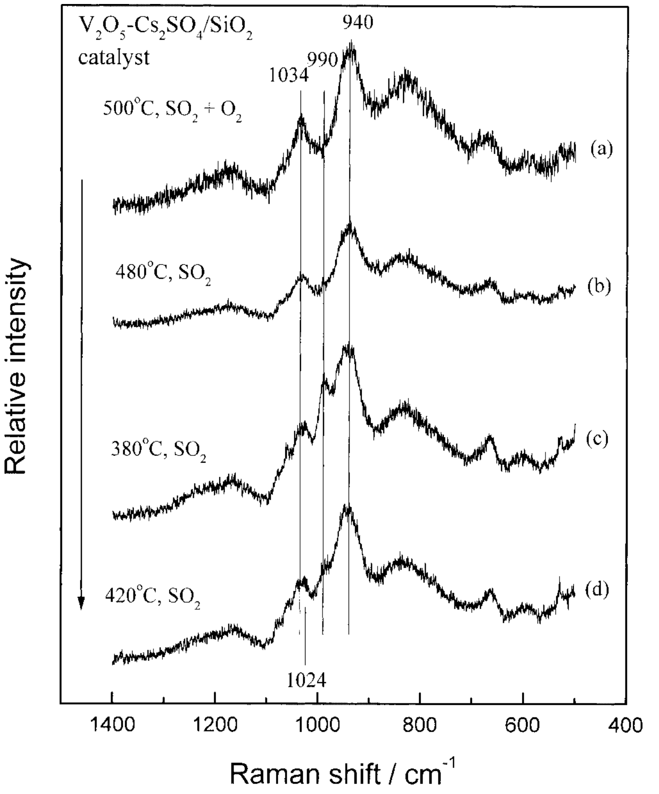

Figure 3. *In situ* Raman spectra of V_2O_5/SiO_2 (6.5 wt% V) impregnated with Cs_2SO_4 ($Cs : V = 3 : 1$) recorded at temperatures and atmospheres listed by each spectrum. Vertical lines mark the positions of the most prominent bands due to the various species (see text). $\lambda_0 = 488.0$ nm, laser power 60 mW, spectral slit width 8 cm^{-1}, scan speed 0.2 cm^{-1} s^{-1}, time constant 1 s.

and (iii) strengthening of the 770/830 cm^{-1} broad feature (bands δ and ε) relative to the 940 cm^{-1} band (band c) of $VO_2(SO_4)_2^{3-}$. These observations indicate the presence of increasing $(VO)_2O(SO_4)_4^{4-}$ amounts at lower temperatures. This may be due to lowering of the reaction rate, giving rise to increased lifetimes of the catalytically active $(VO)_2O(SO_4)_4^{4-}$ complex [3]. Furthermore, freezing of $Cs_2S_2O_7{-}Cs_2SO_4{-}V_2O_5$ melts is known to result in formation of glasses [11–13], which maintain the spectral features of the corresponding melts but the effect on the observed Raman intensities may vary between the two species present (*i.e.*, $VO_2(SO_4)_2^{3-}$ and $(VO)_2O(SO_4)_4^{4-}$). At 300 °C (spectrum 2(e)) the observed bands due to the glassy species are sharper and better resolved. Increasing the temperature to 480 °C under SO_2 and O_2 restores the observed bands of the *in situ* Raman spectrum (shown in figure 2(f)) in their initial relative intensities. The most prominent bands due to the various species present are listed in table 1 (columns 5–8) together with their assignments and are marked by vertical lines in figure 2, where lowercase Greek letters α–θ denote bands due to $(VO)_2O(SO_4)_4^{4-}$. A, B and a–c denote bands due to crystalline Cs_2SO_4 and molten $VO_2(SO_4)_2^{3-}$, as stated before.

Figure 3 shows the *in situ* Raman spectra of the catalysts in the presence of SO_2 (0.4% SO_2 in a balance of N_2), *i.e.*, in reducing conditions. Spectrum (a) is obtained at 500 °C in SO_2/O_2 atmosphere and is identical to spectrum 2(b). After stopping the flow of O_2, no changes are seen in the spectra at 500 and 480 °C (only the spectrum at 480 °C is shown in figure 3(b), for brevity), indicating that the V^V species present are not reduced by SO_2 at these temperatures. However, further lowering of the temperature during exposure to SO_2 results in changes, which are interpreted to indicate reduction of V^V to V^{IV} molten complexes and formation of crystalline V^{IV} compounds. This is seen in figure 3(c) where at 380 °C a sharp band appears at 990 cm^{-1}, characteristic of the $V^{IV}{=}O$ stretch of the vanadyl (VO^{2+}) ion of *crystalline* vanadium compounds [18]. The formation and precipitation of low-valence vanadium crystalline compounds in V_2O_5-based SO_2 oxidation molten salt catalysts have been shown to take place at temperatures typically below 440 °C [19,20]. Previously, the V^{IV} crystalline compounds $Cs_2(VO)_2(SO_4)_3$ and $VOSO_4(SO_2SO_3)_x$ have been isolated from Cs-containing V_2O_5–$Cs_2S_2O_7$ molten salts [19,20]. Depending on the catalyst melt composition and the gas conditions applied, a number of such compounds have been isolated, characterized and referred to as catalyst deactivation products [3,19,20]. When temperature is raised to 420 °C (see spectrum (d) in figure 3) the 990 cm^{-1} almost disappears, indicating the dissolution of the precipitate, as expected [19,20]. The possible $V^V \to V^{IV}$ reactions taking place in the *molten* phase can be written as [13,21]

$$(V^VO)_2O(SO_4)_4^{4-} + SO_2 \to 2V^{IV}O(SO_4)_2^{2-} + SO_3 \qquad (3)$$

$$2V^VO_2(SO_4)_2^{3-} + SO_2 \to V^{IV}O(SO_4)_2^{2-} + V^{IV}O(SO_4)_3^{4-} \qquad (4)$$

The most prominent bands of the V^{IV} *molten* complexes formed according to reactions (3) and (4) are expected in the 935–965 cm^{-1} region [13] (sulfate modes) whereas their $V^{IV}{=}O$ stretch is expected below 1034 cm^{-1} (where the $V^V{=}O$ stretch occurs). Indeed, the V=O band maximum appears to be shifted from 1034 cm^{-1} (spectrum 3(a)) to 1024 cm^{-1} (spectra 3 (c) and (d)).

4. Conclusions

In situ Raman spectroscopy under $SO_2/O_2/SO_3$ atmospheres at temperatures up to 500 °C is used to identify vanadium species on the surface of a Cs-promoted vanadia/silica catalyst (6.5 wt% vanadium and impregnated with Cs_2SO_4, $Cs : V = 3$). The data indicate that (1) the V^V complex $V^VO_2(SO_4)_2^{3-}$ and Cs_2SO_4 dominate the catalyst surface after calcination; (2) under SO_3/O_2 the excess sulfate is converted to pyrosulfate which dissolves the vanadium oxides leading to formation of the V^V dimer $(V^VO)_2O(SO_4)_4^{4-}$ complex; (3) reduction of V^V complexes takes place under SO_2, leading to formation of $V^{IV}O(SO_4)_2^{2-}$ and $V^{IV}O(SO_4)_3^{4-}$. The above-mentioned complex units do not occur necessarily in isolated form but may participate in oligomeric chain-like complex ions

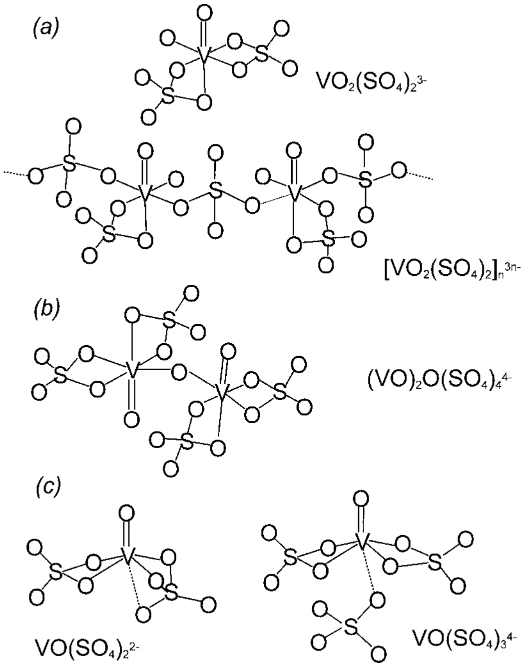

Figure 4. Possible molecular structural models for the V complexes present in the molten salt catalyst: (a) $V^VO_2(SO_4)_2^{3-}$ in monomeric and oligomeric form, (b) $(V^VO)_2O(SO_4)_4^{4-}$ and (c) $V^{IV}O(SO_4)_2^{2-}$ and $V^{IV}O(SO_4)_3^{4-}$.

[3,11–13,20]. Figure 4 shows the proposed structural models for the V species present in the liquid (molten) phase supported on the carrier. The configurations depicted in figure 4 have been deduced earlier, based on high temperature Raman studies of the V_2O_5–M_2SO_4–$M_2S_2O_7$/O_2–SO_2 molten salt/gas systems [11–13]. Significantly, the V^V dimer $(V^VO)_2O(SO_4)_4^{4-}$ has previously been identified as the catalytically active species during SO_2 oxidation in V_2O_5-based molten salt catalysts [3].

This article reports for the first time *in situ* Raman evidence for identifying V species in vanadium-oxide-based SO_2 oxidation catalysts.

Acknowledgment

NATO's Scientific Affairs Division in the framework of the Science for Peace Programme (SfP 971984) has sponsored this research. Support from the General Secretariat of Research and Technology of the Greek Ministry of Development and from FORTH/ICE-HT is gratefully acknowledged.

References

[1] D.J. Smith, Power Eng. Int. (Apr. 21, 1994);
H. Jensen-Holm and O. Rud-Bendixen, Industrial experience with the Topsøe VK 48 sulfuric acid catalyst and the WSA-2 process, presented at *Sulfur 1990*, Cancun, Mexico.
[2] J. Villadsen and H. Livbjerg, Catal. Rev. Sci. Eng. 17 (1978) 203.
[3] O.B. Lapina, B.S. Bal'zhinimaev, S. Boghosian, K.M. Eriksen and R. Fehrmann, Catal. Today 51 (1999) 469.
[4] M.D. Amiridis, I.E. Wachs, G. Deo, J.-M. Jehng and D.S. Kim, J. Catal. 161 (1996) 247.
[5] J.P. Dunn, P.R. Koppula, H.G. Stenger and I.E. Wachs, Appl. Catal. B 19 (1998) 103.
[6] H. Kamata, H. Ohara, K. Takahashi, A. Yukimura and Y. Seo, Catal. Lett. 73 (2001) 79.
[7] G. Went, L.-J. Leu and A.T. Bell, J. Catal. 134 (1992) 492.
[8] G. Went, L.-J. Leu, S.J. Lombardo and A.T. Bell, J. Phys. Chem. 96 (1992) 2235.
[9] I.E. Wachs, G. Deo, B. Weckhuysen, A. Andreini, M.A. Vuurman, M. de Boer and M.D. Amiridis, J. Catal. 161 (1996) 211.
[10] M.D. Amiridis, R.V. Duevel and I.E. Wachs, Appl. Catal. B 20 (1999) 111.
[11] S. Boghosian, F. Borup and A. Chrissanthopoulos, Catal. Lett. 48 (1997) 145.
[12] S. Boghosian, J. Chem. Soc. Faraday Trans. 94 (1998) 3463.
[13] S. Boghosian, A. Chrissanthopoulos and R. Fehrmann, J. Phys. Chem. B, in press.
[14] S.G. Masters, A. Chrissanthopoulos, K.M. Eriksen, S. Boghosian and R. Fehrmann, J. Catal. 166 (1997) 16.
[15] R.M. Caraba, V. Parvulescu, M. Alifanti, V.I. Parvulescu, S. Boghosian, K.M. Eriksen and R. Fehrmann, in preparation.
[16] I. Giakoumelou and S. Boghosian, in preparation.
[17] K. Nakamoto, *Infrared and Raman Spectra of Inorganic and Coordination Compounds* (Wiley, New York, 1986).
[18] J. Selbin, Coord. Chem. Rev. 1 (1966) 293; Chem. Rev. 65 (1965) 153.
[19] S. Boghosian, R. Fehrmann, N.J. Bjerrum and G.N. Papatheodorou, J. Catal. 119 (1989)121.
[20] K.M. Eriksen, D.A. Karydis, S. Boghosian and R. Fehrmann, J. Catal. 155 (1995) 32.
[21] S.B. Rasmussen, K.M. Eriksen and R. Fehrmann, J. Phys. Chem. B 103 (1999) 11282.